Published online 20 May 2015 *Nucleic Acids Research, 2015, Vol. 43, No. 12* ***5971–5983***
doi: 10.1093/nar/gkv539

DNA-PKcs phosphorylates hnRNP-A1 to facilitate the RPA-to-POT1 switch and telomere capping after replication

Jiangdong Sui[1,2], Yu-Fen Lin[1], Kangling Xu[1], Kyung-Jong Lee[1], Dong Wang[2] and Benjamin P.C. Chen[1,*]

[1]Department of Radiation Oncology, University of Texas Southwestern Medical Center, Dallas, TX 75390, USA and [2]Cancer Center, Daping Hospital, Third Military Medical University, Chongqing 400042, China

Received January 14, 2015; Revised May 06, 2015; Accepted May 12, 2015

ABSTRACT

The heterogeneous nuclear ribonucleoprotein A1 (hnRNP-A1) has been implicated in telomere protection and telomerase activation. Recent evidence has further demonstrated that hnRNP-A1 plays a crucial role in maintaining newly replicated telomeric 3′ overhangs and facilitating the switch from replication protein A (RPA) to protection of telomeres 1 (POT1). The role of hnRNP-A1 in telomere protection also involves DNA-dependent protein kinase catalytic subunit (DNA-PKcs), although the detailed regulation mechanism has not been clear. Here we report that hnRNP-A1 is phosphorylated by DNA-PKcs during the G2 and M phases and that DNA-PK-dependent hnRNP-A1 phosphorylation promotes the RPA-to-POT1 switch on telomeric single-stranded 3′ overhangs. Consequently, in cells lacking hnRNP-A1 or DNA-PKcs-dependent hnRNP-A1 phosphorylation, impairment of the RPA-to-POT1 switch results in DNA damage response at telomeres during mitosis as well as induction of fragile telomeres. Taken together, our results indicate that DNA-PKcs-dependent hnRNP-A1 phosphorylation is critical for capping of the newly replicated telomeres and prevention of telomeric aberrations.

INTRODUCTION

Human telomeric DNA is composed of double-stranded repetitive TTAGGG sequences followed by single-stranded G-rich 3′ overhangs, both of which are covered by a telomere-specific shelterin protein complex (1,2). Telomeres adopt a lariat conformation termed the t-loop, in which the telomeric 3′ overhangs hide inside the duplex part of the telomeres. In addition to this architectural exposure protection of telomeric termini, the shelterin complex accumulates at telomeric DNA and establishes a protective nucleoprotein 'cap' for chromosome ends (1,2). Maintenance of the structural integrity of telomeres is necessary to prevent activation of the DNA damage response (DDR) and improper chromosome end-to-end fusion events, which in turn will impair chromosome segregation and cause aneuploidy.

One of the critical issues of telomere maintenance has been the transition between DNA replication and reestablishment of the capping by shelterin at the single-stranded 3′ overhangs. Replication protein A (RPA) complex is the predominant single-stranded DNA binding protein and is essential for both DNA replication and damage repair (3). When replication forks stall, the extension of single-stranded DNA and the coating of RPA trigger activation of ataxia-telangiectasia and Rad3-related (ATR) kinase and DDR (4,5). Thus, it is critical to displace RPA from the newly replicated telomeric 3′ overhangs to prevent unnecessary activation of the ATR signaling pathway at telomeres. Protection of telomeres 1 (POT1), one of the shelterin components, binds to the single-stranded telomeric 3′ overhang and is required for suppression of ATR-dependent DDR (6,7). However, POT1 alone cannot outcompete RPA for the binding of single-stranded telomeric DNA but requires additional support from heterogeneous nuclear ribonucleoprotein A1 (hnRNP-A1) for the RPA-to-POT1 switch. Flynn *et al.* reported that telomeric repeat-containing RNA (TERRA), which traps and modulates the availability of hnRNP-A1 to telomeric DNA, plays a crucial role in orchestrating the RPA-to-POT1 switch for completion of telomere capping (8).

HnRNP-A1 belongs to a large family of hnRNPs (A–U) involved in a diversity of RNA-related processes including alternative splicing, mRNA export, localization, translation and stability (9). Previous studies have also implicated hnRNP-A1 in telomere biogenesis and maintenance. A mouse erythroleukemia cell line lacking hnRNP-A1 expression was found with shortened telomere length, which could be corrected by wild-type hnRNP-A1 or its variant

*To whom correspondence should be addressed. Tel: +1 214 648 1263; Fax: +1 214 648 5995; Email: benjamin.chen@utsouthwestern.edu

termed UP1 carrying only the N′ terminal RNA recognition motifs (RRMs) (10). Subsequent studies demonstrated that hnRNP-A1/UP1 interacts with single-stranded telomeric DNA and the RNA component of telomerase, and can promote telomere length extension through stimulation of telomerase activity (11,12). Together this evidence suggests that hnRNP-A1 is critical for maintenance of telomere length in addition to the RPA-to-POT1 switch and formation of structural protective telomeres (8).

The involvement of hnRNP-A1 in telomere protection has also been linked to DNA-dependent protein kinase (DNA-PK) since hnRNP-A1 interacts with and could be the direct substrate of DNA-PK (13). DNA-PK is composed of the DNA-binding Ku70/Ku80 subunit and the catalytic DNA-PKcs subunit, and is the critical regulator of the non-homologous end-joining pathway of double-stranded break repair (14). Furthermore, Ku70/Ku80 and DNA-PKcs have been linked to telomere protection and maintenance. For example, Ku70/80 has been found to associate with telomeric DNA (15), the human telomere RNA component (hTR) (16), as well as the shelterin TRF1 and TRF2 subunits (17,18). On the other hand, DNA-PKcs is necessary for the prevention of telomere fusions but not for the maintenance of telomere length (19,20), suggesting that DNA-PKcs is needed for the synthesis of the telomere cap structure. The involvement of hnRNP-A1 and DNA-PKcs association in telomere protection came to light as Ting *et al.* reported that hnRNP-A1 is phosphorylated by DNA-PK *in vitro* at Ser95 and Ser192 residues in a DNA- and hTR-dependent manner, and that inhibition of DNA-PK kinase attenuates hnRNP-A1 phosphorylated *in vivo* (13). Furthermore, human VA13 cells that lack hTR display significant reduction in hnRNP-A1 phosphorylation, suggesting that hTR is required for DNA-PK-mediated hnRNP-A1 phosphorylation (13). Consistently, a recent study by Le *et al.* confirmed that DNA-PKcs is required for hnRNP-A1 phosphorylation *in vivo* and that DNA-PK kinase inhibition or hnRNP-A1 depletion results in TERRA accumulation at individual telomeres and increased frequencies of fragile telomeres (21). These evidences also suggest that DNA-PKcs and hnRNP-A1 coordination might play a role in TERRA removal from telomeres, which is needed to facilitate replication of telomeric DNA (22).

Here we demonstrate that there is an increased association between hnRNP-A1 and DNA-PKcs and hnRNP-A1 phosphorylation by DNA-PKcs *in vivo* during the G2 and M phases. Furthermore, DNA-PKcs-dependent hnRNP-A1 phosphorylation could promote the RPA-to-POT1 switch in single-stranded telomeric DNA. Conversely, cells lacking hnRNP-A1 or DNA-PKcs-dependent modification lead to significant sister telomere fusions. Taken together, our results indicate that DNA-PK-mediated hnRNP-A1 phosphorylation is critical for formation of the protective capping structure of newly replicated telomeres to prevent the accumulation of telomeric aberrations.

MATERIALS AND METHODS

Plasmid cloning and mutagenesis

Full-length or truncated hnRNP-A1 cDNAs were amplified from pET9d-hnRNP-A1 (Addgene) and cloned into pcDNA3 vector (Life Technologies) for mammalian expression or pQE-80L vector (Qiagen) for recombinant protein expression in *Escherichia coli*. DNA-PKcs cDNA fragments were cloned into pGEX-6P1 (GE Healthcare Life Sciences) for Glutathione S-transferase (GST) fusion protein expression in *E. coli*. The recently developed CRISPR/Cas9 system was used for targeting the hnRNP-A1 gene and for somatic knockout cell line production (23). In brief, the chimeric single guide RNA (sgRNA) sequences for the hnRNP-A1 gene were chosen accordingly (http://tools.genome-engineering.org). Oligonucleotides carry sgRNA sequences (Supplementary Table S1) that were cloned into pX330-U6-ChimericBB-CBh-hSpCas9 vector (Addgene) for transfection.

Cell culture, treatments and somatic gene knockout

Human colon cancer HCT116 DNA-PKcs$^{-/-}$ (24) and human cervical cancer HeLa cells were maintained in α-MEM (HyClone) supplemented with 10% serum in a humidified incubator at 37°C with 5% CO_2. Cell synchronization with double thymidine or nocodazole was performed as described (25). For kinase inhibitor treatment, 10 μM of Nu7441 or Ku55944 was added to cell culture for 2 h before harvest. Transfection was performed with Lipofectamine 2000 regent (Life Technologies) according to the manufacturer instruction. For hnRNP-A1 gene knockout, HeLa cells were transfected with pX330-hnRNP-A1 and split at 48 h to a density of 0.5 cell per well of a 96-well plate to isolate single-cell-derived clones. The derivative hnRNP-A1 knockout cells were screened by immunofluorescence staining and verified by western blotting. For ectopic expression of hnRNP-A1, hnRNP-A1 knockout cells were transfected with various hnRNP-A1 constructs and subjected to 400 μg/ml G418 treatment for stable cell line selection.

Protein purification and GST pulldown assay

Recombinant his-tagged hnRNP-A1 proteins, RPA complex and GST fusions with DNA-PKcs fragments were expressed in BL21 *E. coli*. Recombinant his-tagged hnRNP-A1 proteins were affinity purified with HisPur Ni-NTA Resin (Thermo Scientific) according to manufacturer's recommendations. Recombinant RPA protein complex was purified as previously described (26). GST fusions cell pellets were lysed and sonicated in STE buffer (150-mM NaCl, 25-mM Tris pH8.0, 1-mM EDTA, 100-μg/ml lysozyme, 1.5% sarkosyl, 2% TX-100), cleared by centrifugation (10 000 rpm for 1 h at 4°C). For GST pulldown, GST lysates were affinity purified with Glutathione-Sepharose beads (GE Healthcare Life Sciences) and incubated with recombinant hnRNP-A1 proteins. Where indicated, biotinylated ss-TEL oligonucleotides (0.5 μM) or ethidium bromide (EtBr) (100 μg/ml) was present during the incubation. Proteins bound to Glutathione-Sepharose beads were analyzed by western blotting.

RPA displacement assay

The RPA displacement assay was modified from the previous protocol (8). In brief, 5 pmol of biotinylated telomeric $(TTAGGG)_8$ or mutant $(TTTGCG)_8$ oligonucleotides (ssTEL or ssMUT, respectively) were incubated with streptavidin-coated magnetic beads (10-mM Tris-HCl pH 8.0, 100-mM NaCl) for 30 min at room temperature (RT), and then incubated with purified RPA (0.2 μg) in binding buffer (10-mM Tris-HCl pH 7.5, 100-mM NaCl, 10-μg/ml BSA, 10% glycerol, 0.05% NP-40) for 30 min at RT. The oligonucleotides coated with RPA were retrieved with a magnet and subsequently mixed with purified recombinant hnRNP-A1 proteins from *E. coli* or indicated nuclear extracts in binding buffer for 30 min at RT. After washes, the remaining bound proteins were analyzed by western blotting.

Electrophoretic mobility shift assay

Electrophoretic mobility shift assay (EMSA) was performed with a Pierce LightShift chemiluminescence EMSA kit with minor modifications. Briefly, the purified proteins or nuclear extracts with or without anti-hnRNP-A1 antibody were incubated with 3′-biotin-labeled single-stranded telomeric DNA probe $(TTAGGG)_8$ or mutated telomeric probe $(TTTGCG)_8$ for 30 min at RT. Samples were separated on a 5% polyacrylamide gel at 100 V for 1 h and then transferred to a Zeta-Probe GT nylon membrane (Bio-Rad). The probes were detected by HRP-conjugated streptavidin and ECL reagents with the kit.

Immunoprecipitation, immunofluorescent staining and western blot

For immunoprecipitation, cell lyses were prepared in lysis buffer (50 mM TrisHCl pH7.5 150mM NaCl, 1% Tween 20, 0.5% NP-40, protease inhibitors), incubated with primary or normal IgG control antibodies for overnight followed by 2 hours incubation with Protein A Sepharose beads (GE Healthcare Life Sciences). Beads were washed with lysis buffer and resuspended in SDS-PAGE loading buffer for western blotting. For immunofluorescent (IF) staining, cells were cultured on glass slides fixed in 4% paraformaldehyde, permeabilized in 0.5% Triton X-100 and blocked in 5% bovine serum albumin. The cells were incubated with primary antibodies for 2 h, followed by Texas Red or Alexa-488-conjugated secondary antibodies (Life Technologies) for 1 h, and then mounted in Vectashield mounting medium with 4, 6-diamidino-2-phenylindole (Vector Labs). Images were acquired from a Zeiss AxioImager M2 microscope system equipped with a Plan-Apochromat 63×/NA 1.40 objective, an AxioCam MRm CCD camera, and AxioVision software (Carl Zeiss). Commercial antibodies were purchased from indicated vendors: phospho-(Ser/Thr) ataxia-telangiectasia mutated (ATM)/ATR substrate antibody, anti-phospho-histone H3, anti-hnRNP-A1, anti-Cyclin A2, anti-Cyclin B1 (Cell Signaling); anti-β-acitn, anti-FLAG M2, anti-His tag, anti- GST tag (Sigma); anti-γ-H2AX, anti-DNA-PKcs (EMD Millipore); anti-RPA2 (Santa Cruz); anti-POT1 (Abcam).

Fluorescence *in situ* hybridization and immuno-fluorescence *in situ* hybridization

Exponentially growing cell cultures were treated with 0.1-μg/ml colcemid for 4 h and were subjected to chromosome spread and fluorescence *in situ* hybridization (FISH) staining as described (27,28). For telomeric FISH (T-FISH), slides were rehydrated in phosphate buffered saline (PBS) for 15 min, treated with 5-mg/ml pepsin for 5 min at 37°C and dehydrated through an ethanol series (70, 85 and 100%). Slides were then incubated with Cy3-labeled C-rich telomeric PNA probe (Panagene) for 2 h at RT, washed in PBS containing 0.02% (v/v) Tween-20 for 15 min at 57°C and then dehydrated again through an ethanol series, air-dried in darkness and mounted with Vectashield mounting medium with DAPI (Vector lab). For chromosome orientation FISH (CO-FISH), cells were cultured in 7.5 mM of 5-bromo-2′-deoxyuridine (BrdU) and 2.5 mM of 5-bromo-2′-deoxycytosine (BrdC) for 20 h prior to colcemid treatment and chromosome spread. Slides were stained with Hoechst 33258 (10 μg/ml), exposed to ultraviolet light (365-nm UV-A, 30 min), incubated with exonuclease III (1.6% v/v, New England Biolabs) for 10 min at RT, hybridized with Cy3-labeled C-rich and fluorescein isothiocyanate-labeled G-rich telomeric PNA probes (Panagene), followed by PBS washes and dehydrated as described. For immuno-FISH, the slides were immunostained with anti-γH2AX antibody and fluorescein-labeled second antibody. After fixation with 4% paraformaldehyde, slides were dehydrated and dried out for T-FISH staining as described.

RESULTS

DNA-PKcs-dependent phosphorylation of hnRNP-A1 *in vivo*

The association between DNA-PKcs and hnRNP-A1 has been implicated in telomere maintenance although there is a lack of *in vivo* evidence. To further investigate the role of DNA-PKcs in hnRNP-A1 regulation *in vivo*, total hnRNP-A1 proteins were immunoprecipitated (IP) from HeLa cells synchronized in different cell cycle phases and were blotted against anti-phospho-SQ/TQ antibody. We observed that hnRNP-A1 protein levels were constant throughout cell cycle phases but hnRNP-A1 phosphorylation increased significantly during G2/M phases (Figure 1A). This G2/M-specific induction of hnRNP-A1 phosphorylation was attenuated in the presence of DNA-PKcs inhibitor Nu7441 but not ataxia telangiectasia mutated (ATM) inhibitor Ku55399 (Supplementary Figure S1). Furthermore, hnRNP-A1 phosphorylation was completely diminished in DNA-PKcs-deficient HCT116 cells (Figure 1B), indicating that DNA-PKcs is the primary kinase responsible for hnRNP-A1 phosphorylation at SQ/TQ motifs during G2/M phases.

DNA-PKcs kinase is able to phosphorylate hnRNP-A1 at the Ser95 and Ser192 residues *in vitro* (13). To validate whether the same phenomenon occurs *in vivo*, HeLa cells were subjected to CRISPR/Cas9-mediated disruption of the endogenous hnRNP-A1 gene (Supplementary Figure S2) and were transiently complemented with flag-tagged wild-type hnRNP-A1 or mutants harboring alanine substitution at Ser95 or Ser192 alone or at both sites. IP-

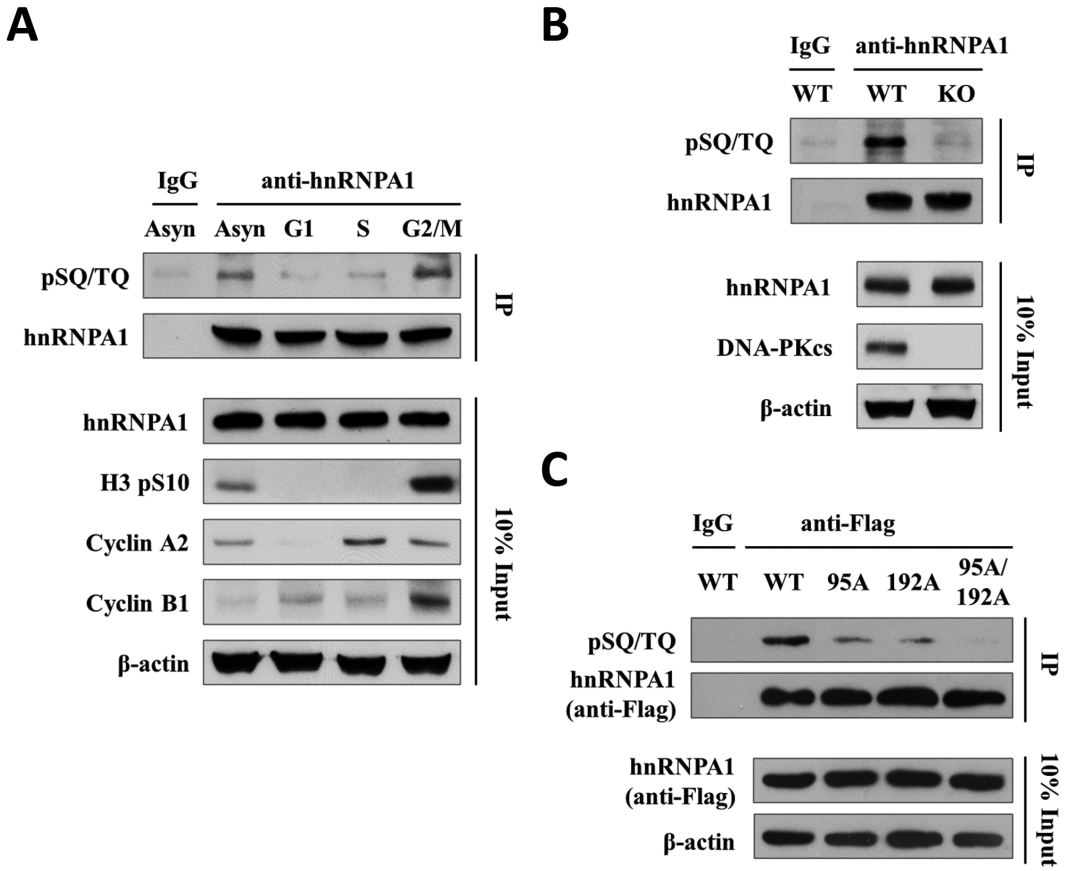

Figure 1. DNA-PKcs phosphorylates hnRNP-A1 *in vivo* during G2/M phases. (**A**) Whole cell lysates from asynchronous and synchronized HeLa cell cultures were immunoprecipitated (IP) with control IgG or anti-hnRNP-A1 antibody, and were western blotted with the indicated antibodies. The phospho-histone H3 (H3 pS10), Cyclin A2 and B1 serve as cell cycle markers. (**B**) Human HCT116 (WT) and derivative DNA-PKcs$^{-/-}$ (KO) cells were synchronized in G2/M and analyzed for hnRNP-A1 phosphorylation status. (**C**) HeLa cells depleted with endogenous hnRNP-A1 using CRISPR/Cas9 strategy were complemented with Flag-tagged full-length hnRNP-A1 (WT) or mutants carrying alanine substitution at Ser95 (S95A), Ser192 (S192A) or both sites (S95A/S192A). Phosphorylation status of hnRNP-A1 was analyzed using G2/M synchronized cell culture as described.

western blot revealed that hnRNP-A1 phosphorylation at SQ/TQ motifs was reduced in S95A and S192A single mutant hnRNP-A1 and was eliminated in S95A/S192A double mutant hnRNP-A1 as compared to wild-type hnRNP-A1 (Figure 1C). These results confirm that Ser95 and Ser192 are main phosphorylation residues of hnRNP-A1 and that hnRNP-A1 is phosphorylated by DNA-PKcs *in vivo* (13,21).

Direct protein–protein interaction between DNA-PKcs and hnRNP-A1 *in vitro* and *in vivo*

Our results indicate that hnRNP-A1 is preferentially phosphorylated by DNA-PKcs during G2/M. Consistent with this notion, we observed that there is an increased association between hnRNP-A1 and DNA-PKcs during G2/M. HeLa cell extracts prepared from asynchronous and nocodazole synchronized cultures were subjected to co-immunoprecipitation (co-IP). In reciprocal co-IP analyses with either anti-DNA-PKcs or anti-hnRNP-A1 antibodies, increased association between DNA-PKcs and hnRNP-A1 was found in nocodazole synchronized extracts (Figure 2A). A similar result was also found in HCT116 cells (Figure 2B), indicating that the interaction between DNA-PKcs and hnRNP-A1 during the G2/M phases facilitates robust phosphorylation of hnRNPA1.

To map the direct protein–protein interaction between DNA-PKcs and hnRNPA1, full-length recombinant hnRNP-A1 proteins (Supplementary Figure S3A) were subjected to GST pulldown assay using a battery of GST fusions with various DNA-PKcs fragments encompassing the entire human DNA-PKcs (Figure 2C). We observed that hnRNP-A1 displays weak association with several DNA-PKcs fragments (A, C, E and F) but interacts primarily with the C-terminus region of DNA-PKcs (a.a. 3747–4128) (Figure 2D), consisting of the kinase domain (KD), phosphatidylinositol-3 kinase-related kinase (PIKK)-regulatory domain (PRD), and FAT-C-terminal (FATC) domain. PRD and FATC domains are present in all PIKK members and are known to mediate protein–protein interaction (29). Further GST pulldown analysis confirmed that hnRNP-A1 preferentially associates with the 'H2' fragment (a.a. 3747–4097) while missing the FACT domain and 'H3' fragment (a.a. 4036–4128) covering both the PRD and FACT domains (Figure 2E), suggesting that the PRD domain in the minimum region of DNA-PKcs interacts with hnRNP-A1. To delineate the minimum re-

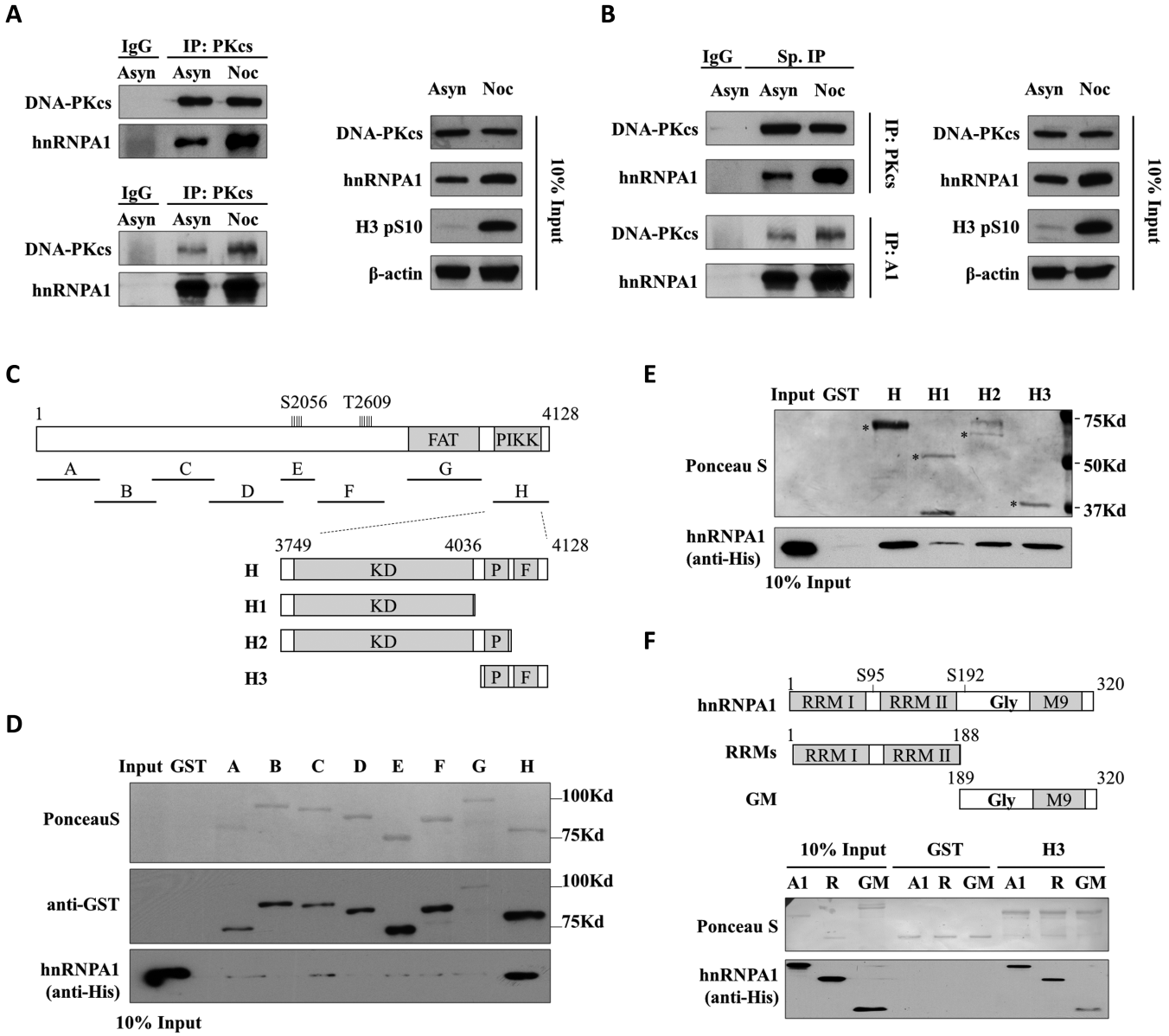

Figure 2. Association between DNA-PKcs and hnRNP-A1 *in vivo* and *in vitro*. (**A**) Asynchronous and nocodazole synchronized HeLa cell lysates were IP with control IgG or specific antibodies against DNA-PKcs (PKcs) or hnRNP-A1 (A1) followed by western blotting. H3 pS10 was used as markers for G2/M synchronization (right panel). (**B**) Similar co-IP analysis was performed in HCT116 cells. (**C**) Schematic of GST fusions with various DNA-PKcs fragments. The C-terminal DNA-PKcs fragment 'H' including the kinase domain (KD), PIKK-regulatory domain (P) and FAT-C-terminal domain (F) was further divided into H1-H3 fragments. (**D**) GST-DNA-PKcs fragments were incubated with His-tagged full-length hnRNP-A1 followed by retrieval with Glutathion-sepharose beads. The bound hnRNP-A1 was western blotted with anti-His antibody (bottom panel). The loading of various GST fusions was demonstrated by Ponceau S staining (top panel) and anti-GST antibody (middle panel). (**E**) DNA-PKcs C-terminal fragments directly interact with full-length hnRNPA1. Asterisks indicate GST-DNA-PKcs fusions by Ponceau S staining (top panel). (**F**) Schematic of hnRNP-A1 contains two RNA binding motifs (RRMs), Gly-rich (Gly) and nucleocytoplasmic shuttling (M9) domains. GST-H3 fusion of DNA-PKcs preferentially interacts with the RRMs (R) but not the Gly-M9 (GM) fragment of hnRNPA1.

gion of hnRNP-A1 for interaction with DNA-PKcs, deletion mutants of hnRNP-A1 including RNA binding motifs (RRMs) and Gly-M9 (GM) domain were bacterially expressed (Supplementary Figure S3A). Further GST pull-down with the GST-H3 DNA-PKcs fragment revealed that the N-terminal RRMs (a.a. 1–188) are the main contributor to the direct protein–protein interaction with DNA-PKcs, although the C-terminal GM domain also displays weak association with DNA-PKcs H3 fragment (Figure 2F). It is interesting to note that RRMs and GM each contain one phosphorylation site of hnRNP-A1. It is possible that hnRNP-A1 phosphorylation might modulate the association between hnRNP-A1 and DNA-PKcs.

HnRNP-A1 phosphorylation facilitates its recruitment to single-stranded telomeric DNA

The N-terminal RRMs of hnRNP-A1 are required for its binding to the single-stranded DNA regions of the telomeric 3′ overhangs (11). To test whether there is competition for hnRNP-A1 binding between DNA-PKcs and telomere 3′ overhangs, single-stranded telomeric DNA oligonucleotides (ssTEL) or mutant oligonucleotides (ssMUT) were tested in GST-H3 pulldown of hnRNPA1. The pulldown analysis revealed that increasing concentrations of ssTEL but not ssMUT interfere with the binding of hnRNP-A1 to the H3 fragment (Figure 3A). Further, addition of EtBr to disrupt protein–DNA association improved GST-H3 pulldown of hnRNP-A1 (Supplementary Figure S3A), indicating that ssTEL and DNA-PKcs compete for the binding of hnRNPA1.

To determine whether DNA-PKcs-dependent hnRNP-A1 phosphorylation modulates the binding of hnRNP-A1 to DNA-PKcs and ssTEL, recombinant hnRNP-A1 mutant proteins harboring a single alanine substitution (non-phospho) or aspartic acid substitution (phospho-mimetic) at either Ser95 or Ser192 were generated (Supplementary Figure S3B). Purified recombinant hnRNP-A1 proteins were incubated with GST-H3 DNA-PKcs fragment and ssTEL followed by a sequential retrieval of the GSH-H3-bound hnRNP-A1 by Glutathione-Sepharose beads and then the ssTEL-bound hnRNP-A1 by the streptavidin-coated beads. We observed that hnRNP-A1 proteins preferentially associate ssTEL and only trace but similar amounts hnRNP-A1 proteins associated with GST-H3 fragment (Figure 3B). In addition, phosphomimetic hnRNP-A1 mutants displayed a stronger binding with ssTEL as compared to wild-type or non-phospho hnRNP-A1 proteins. In parallel experiments, gel mobility shift assay further demonstrated that S95D and S192D mutations augmented hnRNP-A1 binding to ssTEL, whereas S95A and S192A mutations decreased hnRNP-A1 binding to ssTEL (Figure 3C). Collectively, these results suggest that DNA-PKcs-dependent hnRNP-A1 phosphorylation shifts its affinity from DNA-PKcs to single-stranded telomeric DNA.

HnRNP-A1 phosphorylation promotes the RPA-to-POT1 switch at single-stranded telomeric DNA

HnRNP-A1 has been implicated as playing a role in RPA displacement to facilitate the RPA-to-POT1 switch in newly replicated single-stranded telomeric DNA (8). We further investigated whether hnRNP-A1 phosphorylation is required for hnRNPA1-mediated RPA displacement from ssTEL *in vitro* with recombinant hnRNP-A1 proteins. RPA pre-coated ssTEL and ssMUT oligonucleotides were challenged with wild-type, non-phospho, or phosphomimetic hnRNP-A1 proteins for RPA displacement activity. In comparison to wild-type hnRNP-A1 protein, non-phospho hnRNP-A1 mutants were severely impaired in their ability to displace RPA from ssTEL, whereas phosphomimetic hnRNP-A1 proteins displayed enhanced removal of RPA from ssTEL (Figure 4A). In contrast to RPA displacement from ssTEL, neither wild-type nor mutant hnRNP-A1 proteins were able to remove RPA from ssMUT due to sequence-specific binding of hnRNP-A1 to ssTEL but not ssMUT.

RPA displacement activity was further tested using nuclear extracts prepared from control and hnRNP-A1 knockout HeLa cells. Our analysis revealed that hnRNP-A1-deficient nuclear extracts were unable to displace RPA bound to ssTEL as compared to control nuclear extracts; in addition, we observed the loading of POT1 onto ssTEL was significantly attenuated in hnRNP-A1-deficient nuclear extracts (Figure 4B). Both defects in RPA displacement and in POT1 loading of hnRNP-A1 knockout cells were reversed upon complementation with wild-type or phosphomimetic hnRNP-A1 but not with non-phospho mutant hnRNP-A1 (Figure 4C). Phosphomimetic mutants of hnRNPA1, with increased affinity to single-stranded telomeric DNA (Figure 3C), were able to support the loading of POT1 to ssTEL slightly better than wild-type hnRNPA1. Although the ability to displace RPA is likely the reason why hnRNP-A1 supports POT1 loading, we cannot rule out the possibility that there is a direct interaction between hnRNP-A1 and POT1 to facilitate POT1 loading to ssTEL. To test this possible scenario, HeLa nuclear extracts were incubated with GST-hnRNP-A1 fusion protein for pulldown of POT1. However, no binding of POT1 was observed (Supplementary Figure S4B), suggesting that hnRNPA1-mediated RPA displacement is required for POT1 loading to single-stranded telomeric DNA but not association between hnRNPA1and POT1. This is further supported by our analysis showing that hnRNP-A1 bound to ssTEL can be displaced by POT1 in HeLa nuclear extracts over time (Figure 4D). Furthermore, when hnRNPA1-ssTEL was challenged with increasing concentrations of RPA, hnRNP-A1 remained bound to ssTEL regardless of RPA concentrations (Figure 4E). Taken together, these results indicate that single-stranded telomeric DNA can be irreversibly occupied by POT1, but not RPA, in the presence of hnRNPA1.

DNA-PKcs-dependent hnRNP-A1 phosphorylation promotes RPA displacement in single-stranded telomeric DNA

DNA-PKcs-dependent hnRNP-A1 phosphorylation will promote the loading of hnRNP-A1 to single-stranded telomeric DNA for RPA displacement. To determine the specific role of DNA-PKcs in modulating the DNA binding activity of hnRNPA1, nuclear extracts from HCT116 cells and derivative DNA-PKcs$^{-/-}$ cells were tested in gel mobility shift assay with ssTEL and ssMUT oligonucleotides. The specific binding of hnRNP-A1 to ssTEL was demonstrated by the super-shift position in the presence of anti-hnRNP-A1 antibody in DNA-PKcs-proficient HCT116 extracts, and ssTEL binding of hnRNP-A1 was significantly attenuated in extracts prepared from DNA-PKcs$^{-/-}$ cells (Figure 5A). A similar gel mobility shift assay was performed with HeLa nuclear extracts with or without pretreatment with DNA-PKcs kinase inhibitor Nu7441. The result demonstrated that treatment with Nu7441 compromised the binding ability of hnRNP-A1 to ssTEL (Figure 5B). Neither depletion of DNA-PKcs nor Nu7441 treatment affected hnRNP-A1 protein levels, thus excluding the

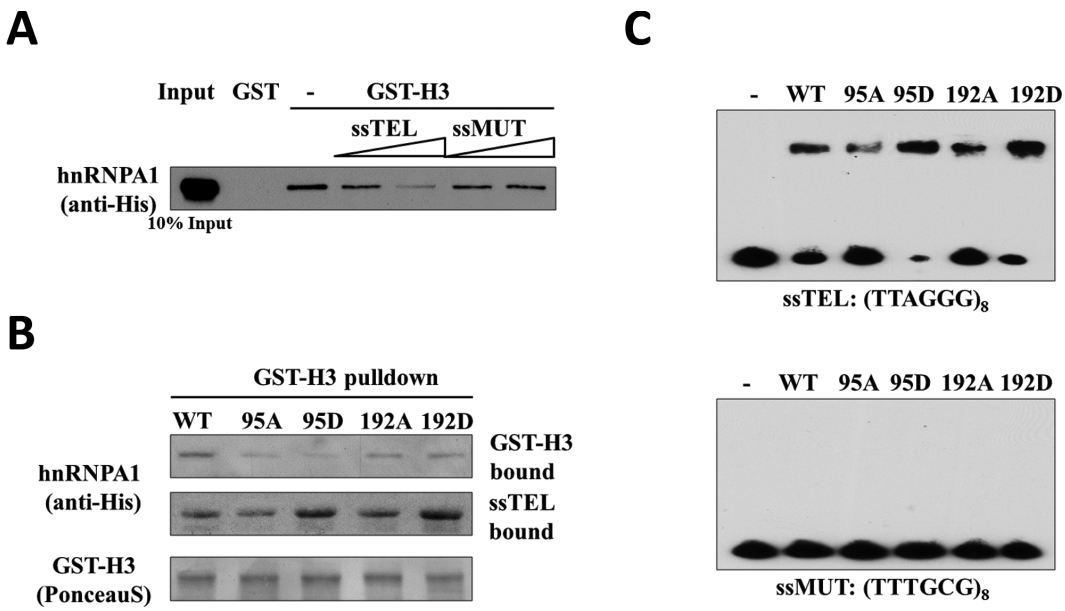

Figure 3. Phosphomimetics facilitate hnRNP-A1 mutants binding to single-stranded telomeric DNA. (**A**) The association between GST-H3 DNA-PKcs fragment and hnRNP-A1 protein was challenged with increasing concentrations (0.2 μM, 2 μM) of either signal-strand telomeric DNA (ssTEL, $TTAGGG_{x8}$) or mutant DNA (ssMUT, $TTTGCG_{x8}$). The bound hnRNP-A1 proteins were western blotted with anti-His antibody. (**B**) WT and mutant hnRNP-A1 proteins were incubated with both GST-H3 fusion protein and biotinylated ssTEL (0.5 μM). GST-H3 bound hnRNP-A1 was retrieved by Glutathion-sepharose beads. The unbound hnRNPA1:ssTEL complex was subsequently retrieved by streptavidin beads and analyzed by western blot. (**C**) Recombinant hnRNP-A1 proteins were incubated with either ssTEL or ssMUT oligonucleotides and analyzed in electrophoretic mobility shift assay (EMSA).

possibility that the alteration was due to a decrease in hnRNP-A1 protein expression (data not shown).

The involvement of DNA-PKcs in hnRNPA1-mediated RPA displacement was further analyzed using nuclear extracts from DNA-PKcs-proficient and deficient cells. Nuclear extracts from DNA-PKcs-proficient HCT116 cells were able to displace RPA bound to ssTEL due to effective loading of hnRNPA1, whereas nuclear extracts from DNA-PKcs$^{-/-}$ HCT116 cells were attenuated in both RPA displacement and hnRNP-A1 loading onto ssTEL (Figure 5C). Consistently, the RPA displacing activity was significantly decreased in HeLa nuclear extracts pretreated with Nu7441 as compared to sham treated nuclear extracts (Figure 5D). Finally, we tested whether phosphomimetic mutants of hnRNP-A1 can bypass the requirement of DNA-PKcs kinase activity and improve RPA displacing activity. Flag-tagged wild-type or phosphomimetic hnRNP-A1 constructs were transfected into HCT116 DNA-PKcs$^{-/-}$ cells. Defect of RPA displacing activity in DNA-PKcs$^{-/-}$ cells was partially restored upon overexpression of S95D or S192D single mutants and was fully restored by S95D/S192D double mutant as compared to that of wild-type HCT116 cells (Figure 5E). The restoration of RPA displacing activity also correlated to the enhanced binding of POT1 to ssTEL. In contrast, overexpression of wild-type hnRNP-A1 was unable to improve RPA displacing activity in DNA-PKcs$^{-/-}$ cells. Furthermore, HeLa cells expressing phosphomimetic hnRNP-A1 mutants, but not wild-type hnRNPA1, were resistant to Nu7441 inhibition and displayed strong RPA displacement similar to untreated control cells (Figure 5F). Taken together, our analyses revealed that phosphomimetic mutants of hnRNP-A1 can restore RPA displacing activity in DNA-PKcs defective cells and that hnRNP-A1 is the downstream effector of DNA-PKcs in regulation of the RPA-to-POT1 switch in single-stranded telomeric DNA.

HnRNP-A1 suppresses telomeric DDR and aberrations

POT1 binding to the single-stranded telomeric 3′ overhangs is required not only for telomere capping but also for preventing ATR-mediated DDR at telomeres (6,7). To determine whether hnRNP-A1 activity also affects DDR, the parental HeLa cells and hnRNP-A1 knockout cells were treated with nocodazole and were subjected to IF staining against γH2AX. Significant γH2AX foci were found in hnRNP-A1$^{-/-}$ cells in mitosis (histone H3 pS10 positive) but not in interphase cells or in wild-type HeLa cells (Figure 6A). The induction of mitotic γH2AX foci in hnRNP-A1$^{-/-}$ cells was suppressed upon expression of wild-type hnRNP-A1 as well as S95D or S192D phosphomimetic mutants but not phospho-dead mutants of hnRNP-A1 (Figure 6B and Supplementary Figure S5), suggesting that hnRNP-A1and its phosphorylation are required for prevention of DDR in mitosis. Our analyses revealed that a great majority of hnRNP-A1$^{-/-}$, S95A and S192A cells displayed significant γH2AX foci (≥3 foci per cell) during mitosis (Figure 6C and D). To verify whether these mitotically occurring γH2AX foci originated at telomeres, HeLa and hnRNP-A1 $^{-/-}$ cells were subjected to mitotic spread and were IF stained against γH2AX in conjunction with T-FISH staining. We observed that these mitotically occurring γH2AX foci indeed overlapped with T-FISH staining (Figure 6E)

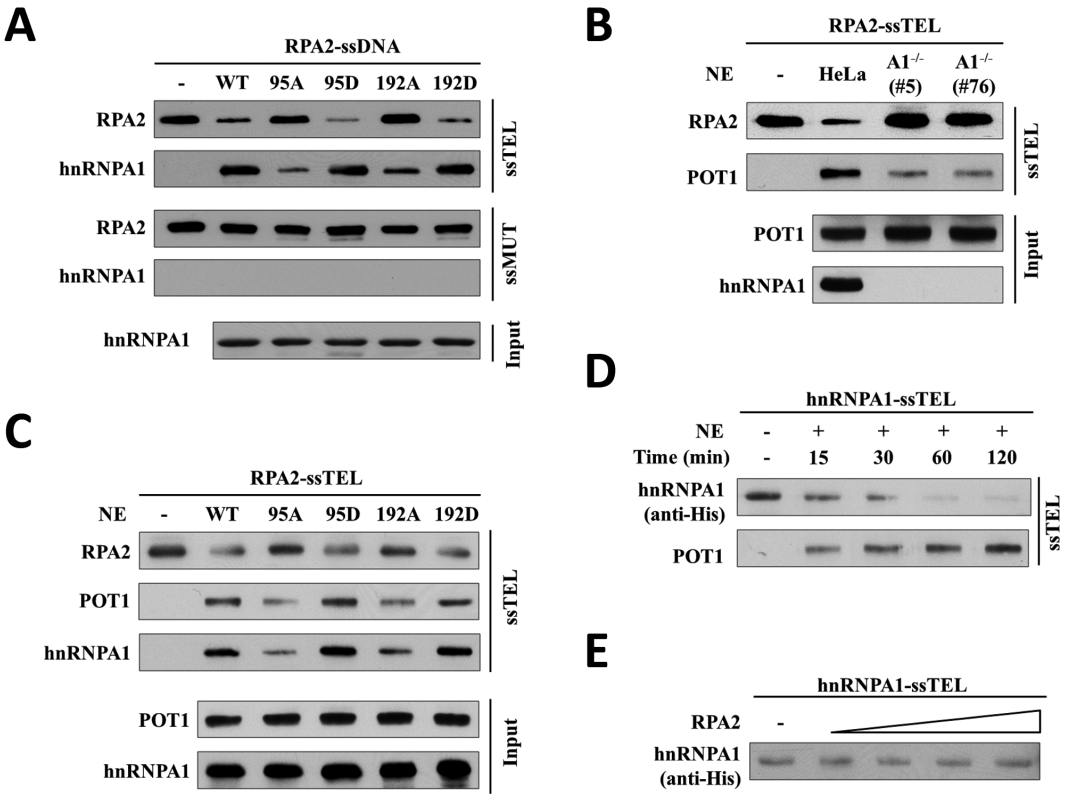

Figure 4. Phosphomimetics enhance hnRNP-A1 ability to displace RPA at single-stranded telomeric DNA. (**A**) RPA-coated ssTEL or ssMUT oligonucleotides were challenged with recombinant WT and mutant hnRNP-A1 proteins. After washing steps, the bound hnRNP-A1 and RPA2 were determined by western blot. (**B**) RPA complexes bound to ssTEL were challenged with nuclear extracts from G2/M synchronized HeLa cells or derivative hnRNP-A1 knockout cells (clones #5 and #76) and were analyzed by western blot. (**C**) HeLa derivative hnRNP-A1$^{-/-}$ cells were complemented with wild type or mutant hnRNP-A1 proteins as indicated. Nuclear extracts made from G2/M synchronized cells were subject to RPA-coated ssTEL analysis as described. (**D**) HnRNPA1-coated ssTEL was incubated with G2/M synchronized HeLa nuclear extracts for different durations as indicated. The bound hnRNP-A1 and POT1 were determined by western blot. (**E**) HnRNPA1-coated ssTEL was treated with increasing concentrations of RPA for 30 min. The remaining ssTEL bound hnRNP-A1 was determined by western blot.

and were significantly higher in hnRNP-A1$^{-/-}$ cells than in HeLa cells (Figure 6F).

Our results revealed that the presence of hnRNP-A1 as well as its phosphorylation is required to suppress the spontaneous DDR at telomeres during mitosis. Consistent with this finding, T-FISH analysis further revealed that significant aberrations were found in hnRNP-A1$^{-/-}$ cells, including telomere-free chromosome ends and sister telomere fusions (Figure 7A). When complemented hnRNP-A1$^{-/-}$ cells with non-phospho S95A or S192A mutant hnRNP-A1, we observed further escalations of all telomere aberrations (Figure 7B), suggesting a dominant negative effect of non-phospho hnRNP-A1 mutants in telomere protection. On the contrary, when complemented with phosphomimetic S95D or S192D mutant hnRNP-A1, telomere aberrations decreased than that of hnRNP-A1$^{-/-}$ cells. However, the frequencies remained higher than that of the parental HeLa cells. Likely, the dynamic regulation of hnRNP-A1 phosphorylation is critical for its role in telomere protection.

To further verify the induction of sister telomere fusions in hnRNP-A1$^{-/-}$ cells, HeLa and hnRNP-A1$^{-/-}$ cells were subjected to CO-FISH analysis, which differentially labels the sister telomeres with G-rich or C-rich telomeric probes (Figure 7C). Our CO-FISH analysis confirmed that significantly more sister telomere fusions occurred in hnRNP-A1$^{-/-}$ cells than in HeLa cells (5.32% versus 0.37%) (Figure 7D). Taken together, these results demonstrate that the role of hnRNP-A1 in the RPA-to-POT1 switch is critical for telomere protection and maintenance of telomere integrity.

DISCUSSION

The multipurpose mRNA splicing factor hnRNP-A1 is also known for its role in telomere maintenance. Early evidence indicated that hnRNP-A1, or its variant UP1 carrying the minimum RNA/DNA binding RRM motifs, interacts with both telomeric DNA and telomerase, facilitates recruitment of telomerase to telomere ends and additionally stimulates telomerase activity and promotes telomere biosynthesis (10–12). Furthermore, hnRNP-A1 binds to telomeric repeat-containing RNA (TERRA) and is able to alleviate TERRA-mediated inhibition of telomerase activity (30). Recent evidence has further indicated that hnRNP-A1 is required for the RPA-to-POT1 switch at the newly replicated single-stranded telomeric DNA and promotes telomere capping (8). DNA-PKcs, on the other hand, is also known to be involved in telomere protection. Independent studies have reported that there is an increase of telomere

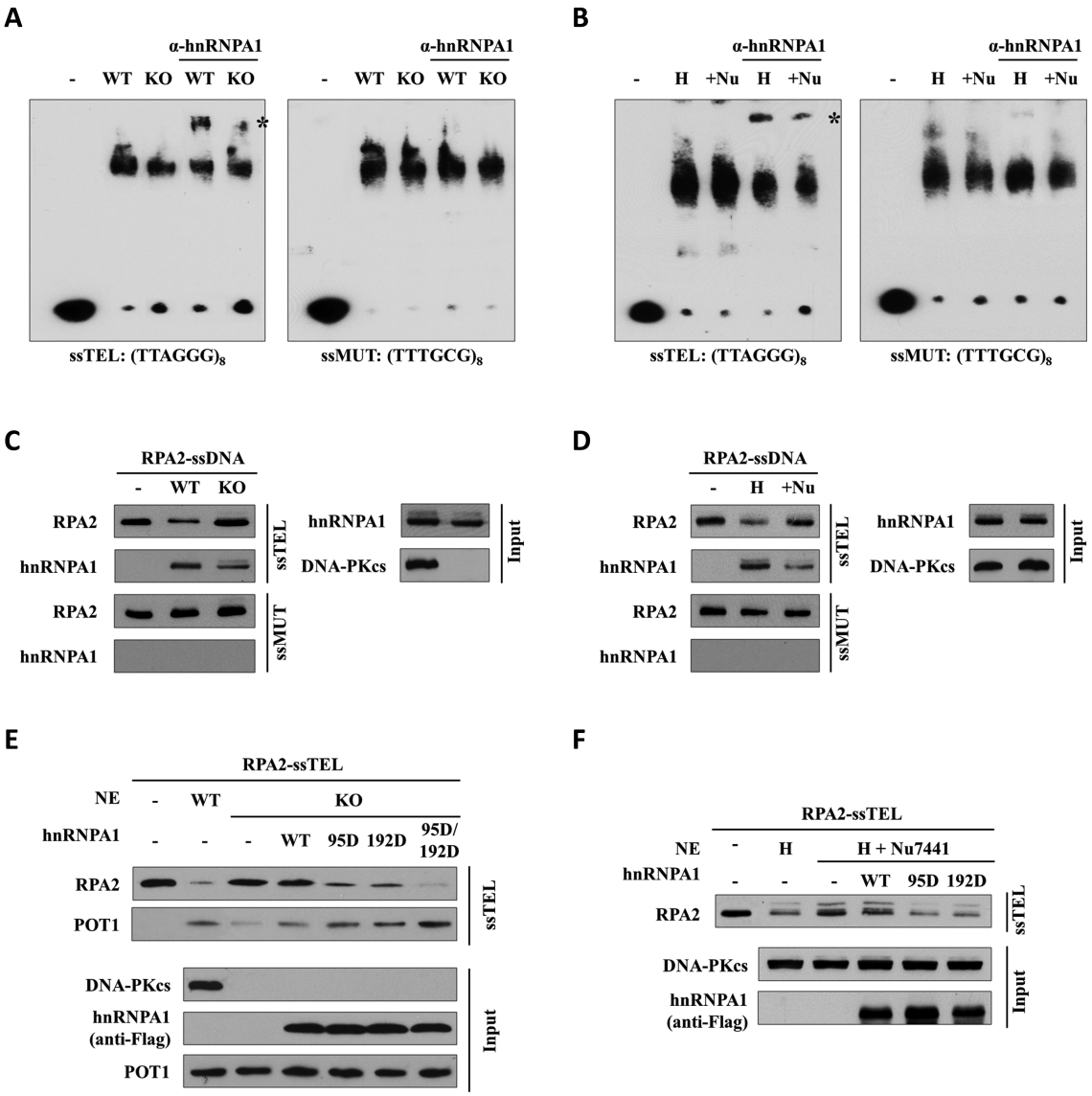

Figure 5. DNA-PKcs-dependent hnRNP-A1 phosphorylation facilitates RPA displacement at single-stranded telomeric DNA. (**A**) Nuclear extracts from G2/M synchronized HCT116 (WT) and DNA-PKcs$^{-/-}$ (KO) cells were incubated with ssTEL or ssMUT oligonucleotides and were analyzed by EMSA assay. Asterisk indicates the super-shifted position of hnRNP-A1-ssTEL in the presence of anti-hnRNP-A1 antibody. (**B**) HeLa cells were synchronized in G2/M with or without Nu7441 treatment for 2 h prior to harvest. Nuclear extracts were subject to EMSA assay as described. (**C,D**) RPA displacing assay was challenged with nuclear extracts from (C) HCT116 and DNA-PKcs$^{-/-}$ cells, or (D) HeLa nuclear extracts with or without Nu7441 pretreatment. (**E**) DNA-PKcs$^{-/-}$ cells were transfected with empty vector, wild type or mutants hnRNP-A1 constructs. G2/M synchronized nuclear extracts were subject to RPA displacing assay. (**F**) HeLa cells transfected with the same hnRNP-A1 expressing constructs were subjected to G2/M synchronization with Nu7441 treatment in the last 2 h. Nuclear extracts were prepared RPA displacing assay.

fusion in mouse DNA-PKcs$^{-/-}$ cells, although DNA-PKcs deficiency does not lead to significant shortening in telomere length, suggesting that DNA-PKcs is mainly involved in telomere capping (19,20,31). Intriguingly, although DNA-PK phosphorylates hnRNP-A1 at Ser95/Ser192 residues *in vitro* (13), it is not clear whether DNA-PK-dependent hnRNP-A1 regulation plays a role in telomere maintenance.

Here we report that DNA-PK kinase is required for hnRNP-A1 phosphorylation *in vivo* during G2 and M phases. We have reported previously that DNA-PK kinase is spontaneously activated upon cell cycle progression through G2/M transition (25). Our current results further demonstrate that there is an increased association between DNA-PKcs and hnRNP-A1 during the G2/M phases and that G2/M-dependent hnRNP-A1 phosphorylation is significantly attenuated in cells lacking DNA-PKcs (Figure 1B) or treated with the DNA-PKcs inhibitor Nu7441 (Supplementary Figure S1). This is consistent with previous studies that DNA-PKcs phosphorylates hnRNP-A1 *in vivo* (13,21). However, we were unable to confirm the requirement of hTR in this regulation (13), as siRNA depletion of hTR in HeLa cells did not alter DNA-PKcs-dependent hnRNP-A1 phosphorylation (Supplementary Figure S6). It is possible that there are additional regula-

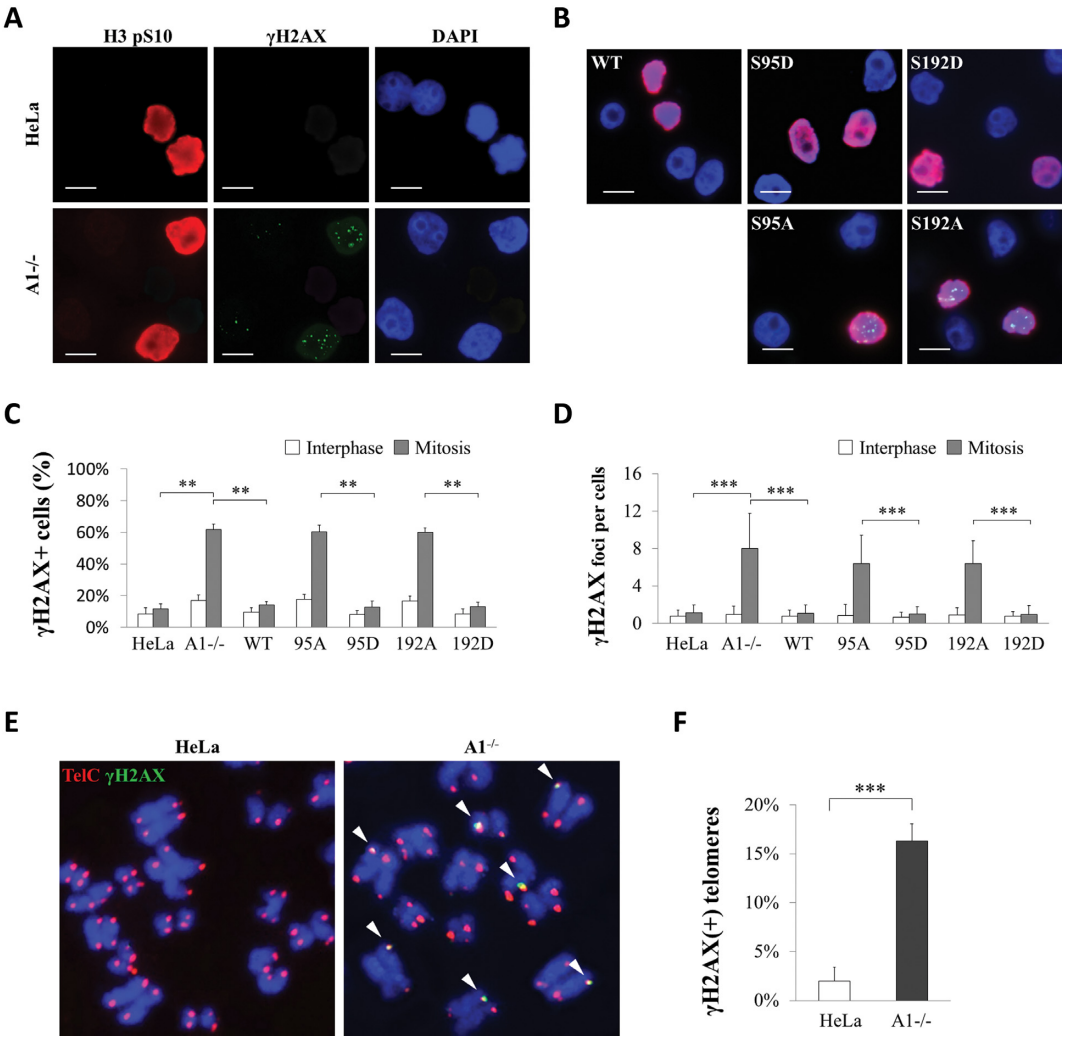

Figure 6. Requirement of hnRNP-A1 in telomere protection after replication. (**A**) HeLa and derivative hnRNP-A1$^{-/-}$ cells treated with nocodazole treatment were immunofluorescent stained against histone H3 pS10 (red) and γ-H2AX (green). Bar represents 10 μm. (**B**) HeLa hnRNP-A1$^{-/-}$ cells complemented with wild type or mutants of hnRNP-A1 were subjected to the same IF staining as described. (**C**) Percentage of γH2AX foci positive cells (≥3 foci) or (**D**) the average numbers of γH2AX foci per cell among HeLa and derivative cells during interphase (H3 pS10 negative) and mitosis (H3 pS10 positive). The results were generated from two independent experiments. $^{**}P < 0.01$; $^{***}P < 0.001$. (**E**) Exponentially growing HeLa and hnRNPA1$^{-/-}$ cells were treated with 0.1-μg/ml colcemid for 4 h and were subjected to mitotic spread. The samples were first immunostained against γH2AX (green) followed by fluorescence *in situ* hybridization (FISH) against C-rich telomeric PNA probe (TelC, red). Arrowheads indicate telomeres positive with γH2AX staining. (**F**) Percentage of γH2AX positive telomeres in HeLa and hnRNP-A1$^{-/-}$ cells. The result was generated from two independent experiments. Greater than 500 chromosomes were analyzed in each experiment. $^{***}P < 0.001$.

tions (e.g. cell type specific) or that residue of hTR after transient siRNA knockdown is sufficient to drive DNA-PKcs-dependent hnRNP-A1 phosphorylation *in vivo*. Consequently, hnRNP-A1 phosphorylation by DNA-PKcs facilitates the binding ability of hnRNP-A1 to single-stranded telomeric DNA to displace RPA for loading of POT1 at single-stranded telomeric DNA. This notion is supported by our findings that inhibition of DNA-PKcs results in decreased binding affinity of hnRNP-A1 to ssTEL oligonucleotides and a defect in RPA displacement (Figure 5) and that phosphomimetic hnRNP-A1 mutant proteins performed better than wild-type or phospho-dead hnRNP-A1 proteins in RPA displacement assay (Figure 4). Of note, RPA is also a critical substrate of DNA-PKcs in DDR (32,33). This raises the question of whether DNA-PKcs-dependent RPA phosphorylation occurs and participates in the RPA-to-POT1 switch. Nonetheless, overexpression of phosphomimetic hnRNP-A1 mutants, but not wild-type or phospho-dead mutant hnRNP-A1, was able to restore the RPA displacement activity in DNA-PKcs-defective cells (Figure 5E and F), strongly indicating that DNA-PKcs-dependent hnRNP-A1 phosphorylation is crucial to the RPA-to-POT1 switch at the newly replicated single-stranded telomeric DNA. This process likely occurs during the late G2 phase when telomere 3′ overhangs are fully processed and mature (34). Defects in this switch would impair telomere capping formation and elicit DDR as evidenced from the surge of telomere-associated γH2AX foci in hnRNP-A1-defective cells (Figure 6E and F).

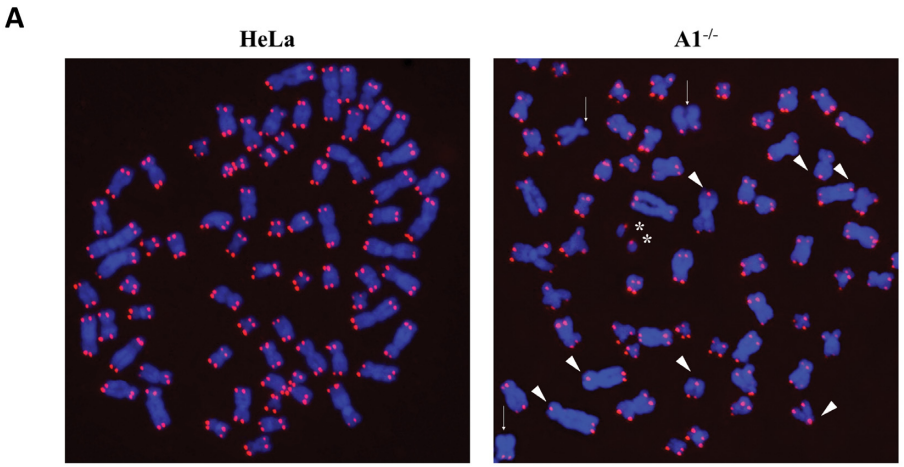

B

	Chrom. No.	Total Abnormal	TFE	AST	TF
Con	2453	23 (0.94%)	9 (0.37%)	9 (0.37%)	5 (0.20%)
A1$^{-/-}$	2488	273 (10.97%)	135 (5.43%)	122 (4.90%)	16 (0.64%)
95A	2074	385 (18.56%)	216 (10.41%)	144 (6.94%)	25 (1.21%)
192A	2049	342 (16.69%)	190 (9.27%)	133 (6.49%)	19 (0.93%)
S95D	1815	79 (4.35%)	47 (2.59%)	23 (1.27%)	9 (0.50%)
S192D	1826	94 (5.15%)	50 (2.74%)	32 (1.75%)	12 (0.66%)

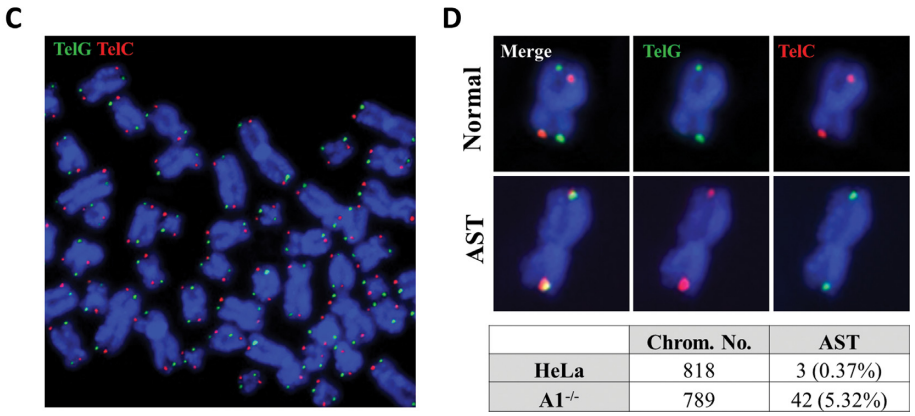

	Chrom. No.	AST
HeLa	818	3 (0.37%)
A1$^{-/-}$	789	42 (5.32%)

Figure 7. Increase of telomere aberrations and sister telomere association in hnRNP-A1-deficient cells. (**A**) Exponentially growing HeLa and hnRNP-A1$^{-/-}$ cells treated with colcemid were subjected to mitotic spread and FISH staining against C-rich telomeric PNA probe (red). Significant telomere aberrations can be found in hnRNPA1$^{-/-}$ cells including telomere-free chromosome ends (TFEs, arrows), associated sister telomeres (ASTs, arrowheads) and telomeric fragments (TFs, asterisks). (**B**) Frequencies of telomeric aberrations observed in the parental HeLa cells, hnRNPA1$^{-/-}$ cells and hnRNPA1$^{-/-}$ cells complemented with various hnRNP-A1 mutants. The result was summarized from two independent analyses. (**C**) Exponentially growing HeLa and hnRNP-A1$^{-/-}$ cells were cultured in BrdU and BrdC containing medium for 20 h and were subjected to chromosome orientation FISH (CO-FISH) staining against C-rich (red) and G-rich (green) telomeric PNA probes. Representative image was generated from control HeLa cells. (**D**) Representative images show patterns of normal and associated sister telomeres. Frequencies of associated sister telomeres in control HeLa and hnRNP-A1$^{-/-}$ cells were quantified based (bottom panel).

RPA is the predominant single-strand DNA (ssDNA) binding protein in mammals and is essential for transient ssDNA protection during DNA replication. On the other hand, the presence of persistent RPA-coated ssDNA filaments upon replication stress or stalled replication forks will lead to recruitment of the ATR-ATRIP (ATR-interacting protein) complex, activation of the ATR signaling pathway and DDR (4,5). The surge of mitosis- and telomere-associated γH2AX foci in hnRNP-A1-defective cells is probably due to an elevation of ATR-dependent DDR signaling. Consistent with this notion, the loss of POT1 also results in the activation of ATR-mediated DDR at telomeres (6,7). Our results demonstrate that DNA-PKcs-dependent hnRNP-A1 phosphorylation is crucial for the prevention of DDR signaling at the newly replicated single-stranded telomeric DNA as the induction of γH2AX foci in hnRNP-A1$^{-/-}$ can be suppressed by wild-type or phosphomimetic hnRNP-A1 mutants but not phospho-dead hnRNP-A1

mutants (Figure 6A and B). These underprotected telomeres and/or mitotic DDR will eventually lead to increases in sister telomere fusions, dicentric chromosomes and aneuploidy (35). Consistent with the above viewpoint, we observed that hnRNP-A1$^{-/-}$ cells possess an elevated number of telomere-associated chromosomal aberrations, particularly telomere-free chromosome ends and sister telomere fusions (Figure 7). Furthermore, complementation with phosphomimetic mutants but not non-phospho mutants decreases telomere aberrations in hnRNP-A1$^{-/-}$ cells, although the frequencies remained higher than that of HeLa cells. It is likely that the dynamic regulation of hnRNP-A1 phosphorylation is critical for its role in the RPA-to-POT1 switch and telomere protection. Taken together, our results demonstrate that the DNA-PK mediation of hnRNP-A1 phosphorylation is critical for maturation of the protective telomere capping structure to preserve the integrity of newly replicated telomeres.

The binding of hnRNP-A1 to single-stranded telomeric DNA does not interfere with the subsequent loading of POT1 as we observed a time-dependent loading of POT1 and diminishing of hnRNP-A1 at ssTEL precoated with hnRNP-A1 (Figure 4D). It is unlikely that the preloading of hnRNP-A1 to single-stranded telomeric DNA would facilitate POT1 recruitment since we did not observe a visible interaction between hnRNP-A1 and POT1 (Supplementary Figure S4B). Conversely, increasing concentrations of RPA were unable to displace hnRNP-A1 preloaded at the ssTEL, suggesting that it is an irreversible process for protein occupancy at newly replicated single-stranded telomeric DNA, starting with the initial RPA-to-hnRNP-A1 switch and followed by the hnRNP-A1-to-POT1 switch. Additionally, a recent study indicates that DNA-PK kinase and hnRNP-A1 could restrict the accumulation of TERRA at telomeres (21), which might facilitate telomeric DNA replication as well as the telomere end-capping process. On the other hand, the surge of TERRA after DNA replication will trap and prevent hnRNP-A1 from binding to single-stranded telomeric DNA, thus favoring the hnRNPA1-to-POT1 switch (8). Conceivably, the dynamic of hnRNP-A1 at telomeres is strictly regulated to govern telomere biosynthesis and formation of capping at the newly replicated telomeres.

Our domain mapping analyses revealed that the RNA/DNA-binding RRM1/2 motifs of hnRNP-A1 mediate the direct interaction with DNA-PKcs (Figure 2). This is consistent with the finding that addition of ssTEL oligonucleotides is able to disrupt the binding of hnRNP-A1 to the DNA-PKcs C′ terminal fragment (Figure 3), suggesting that the similar amino acid residues within RRM1/2 motifs mediate both RNA/DNA-binding and interaction with DNA-PKcs. In addition, the phosphomimetic mutations of hnRNP-A1 improve its association to DNA-PKcs and ssTEL oligonucleotides. It is notable that hnRNP-A1 Ser95 is located within the linker region between the RRM1 and RRM2 motifs, whereas Ser192 is located immediately after the RRM2 motif. It is possible that DNA-PKcs-mediated hnRNP-A1 phosphorylation induces a conformational change of hnRNP-A1 and/or modulates the intermolecular dimerization of hnRNP-A1 (36), thus facilitating the recognition of hnRNP-A1 to single-stranded telomeric DNA.

Domain mapping analyses also reveal that the PRD domain at the DNA-PKcs C′ terminal region is required for hnRNP-A1 association (Figure 2E). The PRD domain and the adjacent FATC domain are conserved in all members of the PIKK family including ATM, ataxia- and Rad3-related (ATR) and DNA-PKcs, and are involved in protein–protein interactions and/or regulation of PIKK kinase activation (29). The PRD domain of DNA-PKcs and ATR has been reported to be involved in stimulatory activation of both kinases (37). Thus, it is possible that the binding of hnRNP-A1 might further stimulate DNA-PKcs kinase activation and/or promote DNA-PKcs-dependent hnRNP-A1 phosphorylation. Our investigation also revealed that the addition of ssTEL oligonucleotides disrupted the interaction between hnRNP-A1 and DNA-PKcs C′ terminal fragment, since the same RRM motifs of hnRNP-A1 are required for both interactions. Thus, it is unlikely that hnRNP-A1 forms a ternary complex with both DNA-PKcs and single-stranded telomeric DNA for recruitment of DNA-PKcs and hnRNP-A1 phosphorylation. This is supported by our finding that DNA-PKcs itself has a low affinity to ssTEL (data not shown). One possible scenario is that DNA-PKcs is being recruited and/or activated at the internal regions of the telomere through Ku heterodimer association with TRF1 (17). DNA-PKcs-dependent hnRNP-A1 phosphorylation will then facilitate hnRNP-A1 binding to single-stranded telomeric DNA and RPA displacement. The indirect tethering of DNA-PK complex to telomeres could prevent improper DDR and end joining of telomeres (17). Besides being regulated by DNA-PKcs, Choi *et al.* have reported that hnRNP-A1 is also phosphorylated by vaccinia-related kinase 1 (VRK1) at Ser6 during the G2/M phases and that VRK1promotes hnRNP-A1 binding to single-stranded telomeric DNA (38). It has yet to be determined whether DNA-PKcs and VRK1 regulate hnRNP-A1 independently or whether there is an upstream–downstream signaling cassette for hnRNP-A1regulation.

In summary, our current studies strongly infer that DNA-PKcs-dependent hnRNP-A1 phosphorylation during G2/M phases promotes the RPA-to-POT1 switch and POT1 loading at newly replicated telomere overhangs for telomere capping. Impairment in this structural protection of telomeres will result in persistence of telomere-associated DDR and accumulation of telomeric aberrations.

SUPPLEMENTARY DATA

Supplementary Data are available at NAR Online.

ACKNOWLEDGEMENT

We thank Dr Marc S. Wold for kindly providing the RPA expression construct and Dee Hill for editing the manuscript.

FUNDING

The National Institutes of Health (NIH) [CA166677 to B.P.C.]; the Cancer Prevention Research Institute of Texas [RP110465 to B.P.C.]; China Scholarship Council

[201207610028 to J.S.]; National Natural Science Foundation of China [81171904 to D.W.]. Funding for open access charge: NIH [CA166677].
Conflict of interest statement. None declared.

REFERENCES

1. de Lange,T. (2009) How telomeres solve the end-protection problem. *Science*, **326**, 948–952.
2. Palm,W. and de Lange,T. (2008) How shelterin protects mammalian telomeres. *Annu. Rev. Genet.*, **42**, 301–334.
3. Wold,M.S. (1997) Replication protein A: a heterotrimeric, single-stranded DNA-binding protein required for eukaryotic DNA metabolism. *Annu. Rev. Biochem.*, **66**, 61–92.
4. Zou,L. (2007) Single- and double-stranded DNA: building a trigger of ATR-mediated DNA damage response. *Genes Dev.*, **21**, 879–885.
5. Zou,L. and Elledge,S.J. (2003) Sensing DNA damage through ATRIP recognition of RPA-ssDNA complexes. *Science*, **300**, 1542–1548.
6. Denchi,E.L. and de Lange,T. (2007) Protection of telomeres through independent control of ATM and ATR by TRF2 and POT1. *Nature*, **448**, 1068–1071.
7. Guo,X., Deng,Y., Lin,Y., Cosme-Blanco,W., Chan,S., He,H., Yuan,G., Brown,E.J. and Chang,S. (2007) Dysfunctional telomeres activate an ATM-ATR-dependent DNA damage response to suppress tumorigenesis. *EMBO J.*, **26**, 4709–4719.
8. Flynn,R.L., Centore,R.C., O'Sullivan,R.J., Rai,R., Tse,A., Songyang,Z., Chang,S., Karlseder,J. and Zou,L. (2011) TERRA and hnRNPA1 orchestrate an RPA-to-POT1 switch on telomeric single-stranded DNA. *Nature*, **471**, 532–536.
9. He,Y. and Smith,R. (2009) Nuclear functions of heterogeneous nuclear ribonucleoproteins A/B. *Cell. Mol. Life Sci.*, **66**, 1239–1256.
10. LaBranche,H., Dupuis,S., Ben-David,Y., Bani,M.R., Wellinger,R.J. and Chabot,B. (1998) Telomere elongation by hnRNP A1 and a derivative that interacts with telomeric repeats and telomerase. *Nat. Genet.*, **19**, 199–202.
11. Fiset,S. and Chabot,B. (2001) hnRNP A1 may interact simultaneously with telomeric DNA and the human telomerase RNA in vitro. *Nucleic Acids Res.*, **29**, 2268–2275.
12. Zhang,Q.S., Manche,L., Xu,R.M. and Krainer,A.R. (2006) hnRNP A1 associates with telomere ends and stimulates telomerase activity. *RNA*, **12**, 1116–1128.
13. Ting,N.S., Pohorelic,B., Yu,Y., Lees-Miller,S.P. and Beattie,T.L. (2009) The human telomerase RNA component, hTR, activates the DNA-dependent protein kinase to phosphorylate heterogeneous nuclear ribonucleoprotein A1. *Nucleic Acids Res.*, **37**, 6105–6115.
14. Davis,A.J., Chen,B.P. and Chen,D.J. (2014) DNA-PK: a dynamic enzyme in a versatile DSB repair pathway. *DNA Repair*, **17**, 21–29.
15. Bianchi,A. and de Lange,T. (1999) Ku binds telomeric DNA in vitro. *J. Biol. Chem.*, **274**, 21223–21227.
16. Ting,N.S., Yu,Y., Pohorelic,B., Lees-Miller,S.P. and Beattie,T.L. (2005) Human Ku70/80 interacts directly with hTR, the RNA component of human telomerase. *Nucleic Acids Res.*, **33**, 2090–2098.
17. Hsu,H.L., Gilley,D., Galande,S.A., Hande,M.P., Allen,B., Kim,S.H., Li,G.C., Campisi,J., Kohwi-Shigematsu,T. and Chen,D.J. (2000) Ku acts in a unique way at the mammalian telomere to prevent end joining. *Genes Dev.*, **14**, 2807–2812.
18. Song,K., Jung,D., Jung,Y., Lee,S.G. and Lee,I. (2000) Interaction of human Ku70 with TRF2. *FEBS Lett.*, **481**, 81–85.
19. Gilley,D., Tanaka,H., Hande,M.P., Kurimasa,A., Li,G.C., Oshimura,M. and Chen,D.J. (2001) DNA-PKcs is critical for telomere capping. *Proc. Natl. Acad. Sci. U.S.A.*, **98**, 15084–15088.
20. Goytisolo,F.A., Samper,E., Edmonson,S., Taccioli,G.E. and Blasco,M.A. (2001) The absence of the dna-dependent protein kinase catalytic subunit in mice results in anaphase bridges and in increased telomeric fusions with normal telomere length and G-strand overhang. *Mol. Cell. Biol.*, **21**, 3642–3651.
21. Le,P.N., Maranon,D.G., Altina,N.H., Battaglia,C.L. and Bailey,S.M. (2013) TERRA, hnRNP A1, and DNA-PKcs interactions at human telomeres. *Front. Oncol.*, **3**, 91.
22. Luke,B. and Lingner,J. (2009) TERRA: telomeric repeat-containing RNA. *EMBO J.*, **28**, 2503–2510.
23. Ran,F.A., Hsu,P.D., Wright,J., Agarwala,V., Scott,D.A. and Zhang,F. (2013) Genome engineering using the CRISPR-Cas9 system. *Nat. Protoc.*, **8**, 2281–2308.
24. Ruis,B.L., Fattah,K.R. and Hendrickson,E.A. (2008) DNA-PKcs regulates proliferation, telomere length and genomic stability in human somatic cells. *Mol. Cell. Biol.*, **28**, 6182–6195.
25. Lee,K.J., Lin,Y.F., Chou,H.Y., Yajima,H., Fattah,K.R., Lee,S.C. and Chen,B.P. (2011) Involvement of DNA-dependent protein kinase in normal cell cycle progression through mitosis. *J. Biol. Chem.*, **286**, 12796–12802.
26. Henricksen,L.A., Umbricht,C.B. and Wold,M.S. (1994) Recombinant replication protein A: expression, complex formation, and functional characterization. *J. Biol. Chem.*, **269**, 11121–11132.
27. Potts,P.R. and Yu,H. (2007) The SMC5/6 complex maintains telomere length in ALT cancer cells through SUMOylation of telomere-binding proteins. *Nat. Struct. Mol. Biol.*, **14**, 581–590.
28. Zhang,S., Yajima,H., Huynh,H., Zheng,J., Callen,E., Chen,H.T., Wong,N., Bunting,S., Lin,Y.F., Li,M. *et al.* (2011) Congenital bone marrow failure in DNA-PKcs mutant mice associated with deficiencies in DNA repair. *J. Cell Biol.*, **193**, 295–305.
29. Lempiainen,H. and Halazonetis,T.D. (2009) Emerging common themes in regulation of PIKKs and PI3Ks. *EMBO J.*, **28**, 3067–3073.
30. Redon,S., Zemp,I. and Lingner,J. (2013) A three-state model for the regulation of telomerase by TERRA and hnRNPA1. *Nucleic Acids Res.*, **41**, 9117–9128.
31. Bailey,S.M., Cornforth,M.N., Kurimasa,A., Chen,D.J. and Goodwin,E.H. (2001) Strand-specific postreplicative processing of mammalian telomeres. *Science*, **293**, 2462–2465.
32. Shao,R.G., Cao,C.X., Zhang,H., Kohn,K.W., Wold,M.S. and Pommier,Y. (1999) Replication-mediated DNA damage by camptothecin induces phosphorylation of RPA by DNA-dependent protein kinase and dissociates RPA:DNA-PK complexes. *EMBO J.*, **18**, 1397–1406.
33. Wang,H., Guan,J., Perrault,A.R., Wang,Y. and Iliakis,G. (2001) Replication protein A2 phosphorylation after DNA damage by the coordinated action of ataxia telangiectasia-mutated and DNA-dependent protein kinase. *Cancer Res.*, **61**, 8554–8563.
34. Chow,T.T., Zhao,Y., Mak,S.S., Shay,J.W. and Wright,W.E. (2012) Early and late steps in telomere overhang processing in normal human cells: the position of the final RNA primer drives telomere shortening. *Genes Dev.*, **26**, 1167–1178.
35. Orthwein,A., Fradet-Turcotte,A., Noordermeer,S.M., Canny,M.D., Brun,C.M., Strecker,J., Escribano-Diaz,C. and Durocher,D. (2014) Mitosis inhibits DNA double-strand break repair to guard against telomere fusions. *Science*, **344**, 189–193.
36. Ding,J., Hayashi,M.K., Zhang,Y., Manche,L., Krainer,A.R. and Xu,R.M. (1999) Crystal structure of the two-RRM domain of hnRNP A1 (UP1) complexed with single-stranded telomeric DNA. *Genes Dev.*, **13**, 1102–1115.
37. Mordes,D.A., Glick,G.G., Zhao,R. and Cortez,D. (2008) TopBP1 activates ATR through ATRIP and a PIKK regulatory domain. *Genes Dev.*, **22**, 1478–1489.
38. Choi,Y.H., Lim,J.K., Jeong,M.W. and Kim,K.T. (2012) HnRNP A1 phosphorylated by VRK1 stimulates telomerase and its binding to telomeric DNA sequence. *Nucleic Acids Res.*, **40**, 8499–8518.